Thermal reactivities of catechols/pyrogallols and cresols/xylenols as lignin pyrolysis intermediates

AUTHOR(S):

Asmadi, Mohd; Kawamoto, Haruo; Saka, Shiro

CITATION:

Asmadi, Mohd ...[et al]. Thermal reactivities of catechols/pyrogallols and cresols/xylenols as lignin pyrolysis intermediates. Journal of Analytical and Applied Pyrolysis 2011, 92(1): 76-87

ISSUE DATE:

2011-09

URL:

http://hdl.handle.net/2433/147229

Thermal Reactivities of Catechols/Pyrogallols and Cresols/Xylenols as Lignin Pyrolysis Intermediates

Mohd Asmadi, Haruo Kawamoto*, Shiro Saka

Graduate School of Energy Science, Kyoto University
Yoshida-honmachi, Sakyo-ku, Kyoto 606-8501, Japan

*Corresponding author: Tel/Fax: +81-75-753-4737
Email address: kawamoto@energy.kyoto-u.ac.jp

Abstract

Thermal reactivities of lignin pyrolysis intermediates, catechols/pyrogallols (O-CH_3 homolysis products) and cresols/xylenols (OCH_3 rearrangement products), were studied in a closed ampoule reactor (N_2/ 600 °C/ 40–600 s) to understand their roles in the secondary reactions step. Reactivity tends to be enhanced by increasing the number of substituent groups on phenol and this effect was greater for -OH than for -CH_3. Thus, catechols/pyrogallols were more reactive than cresols/xylenols and syringol-derived products were more reactive than corresponding guaiacol-derived products. Catechols/ pyrogallols were effectively converted into CO (additionally CO_2 in the case of pyrogallols) in the early stage of pyrolysis. In contrast, cresols/xylenols were comparatively stable and produced H_2, CH_4 and demethylation products (cresols and phenol) after prolonged heating. All intermediates except phenol and 2-ethylphenol formed coke during a long heating time of 600 s (second stage coking). Based on the present results, the roles of intermediates in tar, coke and gas formation from guaiacol and syringol are discussed at the molecular level, focusing on their differences. Molecular mechanisms of gas formation from pyrogallols and demethylation of cresols/ xylenols are also discussed.

Keywords:

Pyrolysis; gasification; coking; lignin; aromatic structure; intermediate

1. Introduction

Lignin aromatic structure varies between wood species. Hardwood lignin contains guaiacyl (4-hydroxy-3-methoxyphenyl) and syringyl (3,5-dimethoxy-4-hydroxyphenyl) structures, while the guaiacyl-type is predominant in softwood lignin [1,2]. Because of such differences in substitution pattern of the aromatic rings, softwood and hardwood lignins form different types of pyrolytic products. The GC/MS studies of the primary pyrolysis products from hardwood lignins [2–7] indicate the formation of guaiacol (2-methoxyphenol) and syringol (2,6-dimethoxyphenol) and their derivatives with various saturated, >C=C< and >C=O side-chains at their C4-positions. Only guaiacol and its derivatives form from softwood lignins.

These primary products are subjected to secondary reactions [2–7]. Catechols/pyrogallols, cresols/xylenols, phenol, polyaromatic hydrocarbons (PAHs), coke and gas are reported as the secondary products [8–17]. Two competitive reactions, i.e., O-CH_3 bond homolysis [18] and radical-induced OCH_3 rearrangement (*ipso* substitution) [18], are known to be important secondary reaction pathways. These reactions change the aromatic OCH_3 structure into aromatic OH (catechols/pyrogallols) and CH_3 (cresols/xylenols), respectively. Phenol is formed via decarbonylation of an aldehyde derivative formed in the course of the OCH_3 rearrangement pathway [18].

In our previous study [19], the secondary reaction behaviors of lignin during softwood and hardwood pyrolysis were compared using an ampoule reactor (N_2/ 600 °C). Syringol and its derivatives were obtained from Japanese beech (*Fagus crenata*, a hardwood) along with the corresponding guaiacol derivatives during a brief heating time. The composition suddenly changed and became similar to that of Japanese cedar (*Cryptomeria japonica*, a softwood) during prolonged heating, mostly attributed to the guaiacyl unit. More extensive coking was also observed for Japanese beech.

The subsequent comparative study of guaiacol and syringol pyrolysis as model aromatic nuclei of lignin under similar pyrolysis conditions [20] revealed that these features are characteristic of the aromatic ring moieties. In the two-stage coking observed during pyrolysis of guaiacol and syringol, the amount of the first-stage coke formed during a brief heating time was almost double in the latter sample, which, in turn, led to a lower GC/MS-detectable tar yield. This is explained by the double opportunity of the OCH_3 rearrangement pathway in syringol, which possesses an additional OCH_3 group. *o*-Quinonemethide intermediates, which are proposed as key intermediates for coke formation [21], are formed in the course of this rearrangement pathway. Additionally, higher gas yields (especially CH_4 and CO_2), greater secondary decomposition reactivities of the intermediates, and lower yields of anthracene and phenanthrene as PAHs, were suggested for syringol. These are expected to arise from the different reactivities of the pyrolysis intermediates formed from syringyl and guaiacyl units.

Several papers describe the thermal decomposition of catechols, phenols [8–13] and cresols/xylenols [14–17]. However, thermal decomposition behaviors including coking and gas formation have not been compared for guaiacyl- and syringyl-derived pyrolysis

intermediates. In this paper, thermal reactivities of lignin pyrolysis intermediates, catechols/pyrogallols, cresols/xylenols and phenol, are described, focusing on the differences between guaiacyl- and syringyl-derived compounds. The roles played by these intermediates in coke, gas and tar formation during lignin pyrolysis are also discussed.

2. Experimental

2.1. Materials

Phenol (**1**), pyrocatechol (benzene-1,2-diol, **2**), 3-methoxycatechol (3-methoxybenzene-1,2-diol, **3**), 4-methylcatechol (4-methylbenzene-1,2-diol, **4**), 3-methylcatechol (3-methylbenzene-1,2-diol, **5**), pyrogallol (benzene-1,2,3-triol, **6**), 5-methylpyrogallol (5-methylbenzene-1,2,3-triol, **7**), *o*-cresol (2-methylphenol, **8**), 2-methoxy-6-methylphenol (**9**), 2,3-xylenol (2,3-dimethylphenol, **10**), 2,4-xylenol (2,4-dimethylphenol, **11**), 2,6-xylenol (2,6-dimethylphenol, **12**), 2,4,6-trimethylphenol (**13**) and 2-ethylphenol (**14**) were used as lignin pyrolysis intermediates (Fig. 1). These were purchased from Nacalai Tesque Inc., Kyoto as guaranteed grades. Compounds **2**-**5** and **6**-**7** are the catechol and pyrogallol derivatives, respectively, and both are the products of the O-CH_3 bond homolysis pathway. Cresol **8** and xylenols **10**–**13** are formed through the OCH_3 rearrangement pathway. Compound **5** is a product formed through both pathways. Syringyl-characteristic compounds **3**, **5**–**7**, **9**, **12** and **13** have generally more substituent groups (OH and CH_3) than the guaiacyl-characteristic compounds **1**, **2**, **4**, **8**, **10**, **11** and **14**. Compounds **3** and **9** have one OCH_3 group.

2.2. Pyrolysis and product analysis

Each sample (10 mg) was placed at the bottom of Pyrex glass ampoule. After the air inside the glass ampoule was exchanged with N_2 by using an aspirator, the glass ampoule was sealed. The sealed ampoule reactor was then heated for 40–600 s in an upright orientation in a muffle furnace preheated at 600 °C. The ampoule was immediately cooled by flowing air for 1 min and opened with a gas collecting apparatus according the method described in the literature [22]. After collecting the gaseous products, residuals inside of the ampoule reactor were extracted with MeOH (1.0 mL × 2) to obtain MeOH-soluble (tar) and MeOH-insoluble (coke) fractions. In this paper, a black carbonaceous solid substance observed on the upper side of the reactor wall was defined as coke. The coke yield was determined from the weight change of the glassware after incineration of coke in air at 600 °C for 2 h. According to the temperature profiles reported in our previous paper [20], it took about 120 s for the inside temperature to reach the furnace temperature.

Non-condensable gases were determined by Micro GC using a Varian CP-4900 instrument under the following conditions; channel 1) column: MS5A 10 m; carrier gas: argon; column temperature: 100 °C; column pressure: 170 kPa; detector: thermal

conductivity detector (TCD); retention times (s): H_2 (26.4), N_2 (45.7), O_2 (35.4), CH_4 (60.6) and CO (86.9); channel 2) column: PoraPLOT Q 10 m; carrier gas: helium; column temperature: 80 °C: column pressure: 190 kPa; detector: thermal conductivity detector (TCD); retention time (s): CO_2 (19.9).

MeOH-soluble fractions were analyzed by GC-MS for determination of the low MW products. Identification of the products was conducted according to the previous papers [19, 22, 23]. The yields of low MW products were determined from the total-ion chromatograms by comparing their peak areas with that of *p*-dibromobenzene as an internal standard. The analysis was carried out using a Hitachi G-7000 gas chromatograph and a Hitachi M9000 mass spectrometer under the following conditions; column: Shimadzu CBP-M25-O25 (length: 25 m, diameter: 0.25 mm); injector temperature: 250 °C; column temperature: 40 °C (1 min), 40 → 300 °C (1 → 53 min), 300 °C (53 → 60 min); carrier gas: helium; flow rate: 1.5 ml/min; emission current: 15 µA; ionization time: 100 ms.

All experiments were repeated 3 times and yields of the products observed were similar amongst the replicates, although the data were not treated statistically.

3. Results and discussion

3.1. Structure - reactivity relationship

Reactivities suggested by the recoveries of compounds **1**, **2**, **4**–**8**, **10**–**14** during pyrolysis (N_2/ 600 °C/ 80–600 s) are shown in Fig. 2. Lower recovery means higher decomposition reactivity and *vice versa*. Although phenol (**1**) was fairly stable, the reactivity was found to increase with the number of substituent groups (OH and CH_3) as follows: phenol (**1**, 1 OH) < catechols **2**, **4** and **5** (2 OH) < pyrogallols **6** and **7** (3 OH) for catechols/syringols; phenol < *o*-cresol (**8**, 1 CH_3) < 2,3-xylenol (**10**, 2 CH_3), 2,4-xylenol (**11**, 2 CH_3) < 2,6-xylenol (**12**, 2 CH_3), 2,4,6-trimethylphenol (**13**, 3 CH_3) for cresols/xylenols. The influence of OH was generally greater than that of CH_3. Thus, the O-CH_3 homolysis products **2**, **4**–**7** with OH substituents were more reactive than the OCH_3 rearrangement products **1**, **8**, **10**–**13** with CH_3. We found in previous studies that the GC/MS-detectable tar became a mixture of cresols, phenol and PAHs after a long heating time during the pyrolysis of softwood/hardwood [19] and guaiacol/syringol [20]. These observations probably arise from the higher decomposition reactivities of catechols/pyrogallols.

The syringyl-characteristic compounds **5**–**7**, **12** and **13**, which have more substituent groups (OH and/or CH_3), had generally greater reactivity than the guaiacyl-characteristic compounds **1**, **2**, **4**, **8**, **10** and **11**. Such reactivity differences reasonably explain our previous observation [19, 20] that the syringyl-characteristic intermediates tend to disappear more rapidly than guaiacyl-characteristic intermediates and would be converted into other products more effectively.

Yields of gas and MeOH-soluble and MeOH-insoluble (coke) fractions are summarized in Fig. 3. Gas formation from catechols/pyrogallols **2**, **4**–**7** started from a short heating time of 80 s and their yields reached 39.4–73.9 wt% at 600 s. Pyrogallols **6** and **7**, in particular, produced large amounts of gas. Contrary to this, cresols/xylenols **8**, **10**–**13** and 2-ethylphenol (**14**) were comparatively stable for gas formation and their gas yields at 80 and 120 s were negligible. Only small amounts (4.6–13.0 wt%) of gas were observed from these compounds after a longer heating time of 600 s. From the temperature-dependency data (Fig. 4) under similar conditions (120 s), gas formation from pyrocatechol (**2**) and pyrogallol (**6**) started at around 500–600 °C. This is a similar temperature range to that where gas formation from guaiacol and syringol became significant [20]. Consequently, catechols/pyrogallols are suggested to be key intermediates for gas formation from guaiacol/syringol. Higher gas formation reactivities of pyrogallols than those of catechols probably account for the higher gas yield from syringol than guaiacol in our previous paper [20].

Coke formation behaviors also differed between catechols/pyrogallols and cresols/xylenols. The former compounds produced small amounts of coke even at 80 s and yields increased with increasing heating time. In contrast, no coke was formed from cresols/xylenols at 80 and 120 s, while their coke formation became significant at 600 s (6–24 wt%). Thus, some induction period exists for coke formation from cresols/xylenols. Phenol (**1**) and 2-ethylphenol (**14**) did not form coke, even at 600 s.

3.2. Two stage coking

Pictures of the ampoule reactors after tar extraction and MeOH-soluble tar fractions obtained after pyrolysis are given in Fig. 5. Pictures published previously for pyrolysis of guaiacol (**15**) and syringol (**16**) [20] are also included. We found in the previous work [20] that coking occurred in two stages depending on the heating time during pyrolysis of guaiacol and syringol. Syringol produced much greater amounts (almost double) of 1st stage coke than guaiacol at relatively short heating times of 80 and 120 s. Additional coke occurred during a longer heating time of 600 s (2nd stage coking). Because 3-methoxycatechol (**3**) and 2-methoxy-6-methylphenol (**9**), which are the intermediates from syringol containing one OCH_3 group, formed significant amounts of coke at 80 s, the higher 1st stage coking reactivity of syringol was explained by the double opportunity for the OCH_3 rearrangement pathway [20]. Hosoya et al. [21] proposed an *o*-quinonemethide as a key intermediate for coking, which is formed in the course of the OCH_3 rearrangement pathway. In the present study, the 1st stage coking reactivity was clearly shown to vary depending on the compound type in the following order: compounds **3** and **9** with OCH_3 group > catechols/pyrogallols > cresols/xylenols, phenol and 2-ethylphenol. These observations confirm the above proposed mechanism.

At 600 s, all compounds except phenol (**1**) and 2-ethylphenol (**14**) formed significant amounts of coke (2nd stage coke). Accordingly, these pyrolysis intermediates are suggested to be precursors of 2nd stage coking. It should be noted that the coking

reactivity is quite dependent on the alkyl structure in alkyl phenols. From the comparison between phenol (**1**), 2-ethylphenol (**14**) and cresols/xylenols **8**, **11**–**1**3, only cresols/xylenols with methyl substituents were reactive in the 2nd stage coking. Interestingly, the coke yield increased with an increase in the number of methyl groups (Fig. 3): *o*-cresol (6.1 wt%) < 2,4-xylenol (12.8 wt%), 2,6-xylenol (9.2 wt%) < 2,4,6-trimethylphenol (23.5 wt%). These results strongly suggest that the reactivity of cresols/xylenols for 2nd stage coking is directly related to the number of methyl groups. *o*-Quinonemethide intermediates would be possible also formed from methylated phenols through abstraction of phenolic and benzylic hydrogens (Fig. 6). Such *o*-quinonemethide formation may be involved in this coking. This radical-induced reaction can also explain the induction period observed for coking of cresols/xylenols. A similar influence of alkyl group on 1st stage coking reactivity was reported by Hosoya et al. [21]. They found that 2-ethoxyphenol did not form coke, although 2-methoxyphenol (*o*-cresol) formed significant amounts of coke under similar conditions.

Coking reaction of catechols/pyrogallols may proceed in a different manner. There is a large volume of literature [8–9, 24–27] dealing with the thermal decomposition of phenol and catechol, focusing on PAH formation. A cyclopentadienyl radical is proposed as an important precursor of PAH [28–30]. This radical was also reported in the pyrolysis of catechol [12]. Such reactive intermediate formation would be involved in the coking mechanisms of catechols/pyrogallols.

3.3. Color of MeOH-soluble fractions

Coloration and decoloration behavior of MeOH-soluble fractions varied depending on the intermediate structure (Fig. 5). During pyrolysis of guaiacol and syringol, the color of the soluble portions became dark brown and then decolorized with increasing pyrolysis time. Finally, the color became light yellow at 600 s. This tendency was more pronounced with syringol.

Catechols/pyrogallols tend to produce dark color solutions in the early stage of pyrolysis (80 s), whereas the solutions obtained from cresols/xylenols were almost colorless. Thus, catechols/pyrogallols decomposition may be a reason for the severe coloration at 80 and 120 s during pyrolysis of guaiacol/syringol. The syringol-characteristic intermediates **5**–**7** were more pronounced in this coloration than the guaiacol-characteristic intermediates **2** and **4**.

With increasing the pyrolysis time to 600 s, most of the solutions from catechols/pyrogallols were decolorized. In contrast, cresols/xylenols produced yellow solutions. Change in the solution color during pyrolysis of guaiacol/syringol is reasonably explained as the sum of the results of these pyrolysis intermediates.

3.4. Gaseous products

Formation behavior of each gaseous component (H_2, CH_4, CO and CO_2) during pyrolysis is shown in Fig. 7. Gas composition varied depending on the chemical structure

of the intermediates and pyrolysis time. Catechols/pyrogallols **2**,**4**,**6** and **7** formed large amounts (29.9–41.4 wt% at 120 s) of CO in the early stage of pyrolysis (≈120 s) and the formation slowed down in the period 120–600 s. Only pyrogallols **6** and **7** gave CO_2 in significant yields (6.1 and 6.2 wt%, respectively, at 120 s), and this formation was also almost complete before 120 s. The yield (34.5 wt%) of CO from pyrocatechol (**2**) at 600 s corresponds to 67.7% of the oxygen atoms in the molecule. Interestingly, in the case of pyrogallol (**6**), this value reached almost 100%; 85 and 15% of the oxygen atoms in the molecule were converted into CO (58.7 wt%) and CO_2 (8.2 wt%), respectively, at 600 s (number in parenthesis: yield from **6**). Accordingly, large proportions of the oxygen atoms in catechols/pyrogallols are converted into the gaseous products under the present conditions. This is not the case for cresols/xylenols.

The CO and CO_2 yields from cresols/xylenols **8**, **11**–**13** were almost negligible. The oxygen atoms in cresols/xylenols do not generate gaseous products under the present conditions. In contrast, H_2 and CH_4 were the major gas components arising from these compounds. Similar yields of H_2 and CH_4 were also observed from catechols/pyrogallols. Unlike the CO and CO_2 formation from catechols/pyrogallols, formation of H_2 and CH_4 occurred at rather longer pyrolysis times between 120-600 s.

It should be noted that the CH_4 yield was directly related to the number of methyl groups in cresols/xylenols, where the yield increased in the order: *o*-cresol (**8**, 2.8 wt %) < 2,4-xylenol (**11**, 5.9 wt %), 2,6-xylenol (**12**, 6.0 wt %) < 1,3,5-trimethylphenol (**13**, 9.5 wt %). These results suggest that the CH_4 originates from the methyl group in these molecules. With this assumption, the CH_4 yields correspond to 19.0–27.0% of the methyl group contents in these compounds. This CH_4 formation is probably related to the demethylation reaction, as discussed below.

Formation of CO from catechols may be explained using the mechanisms proposed for phenol [31, 32], phenoxy radical [33–36] and catechol [8]. Harrison et al. [37] found that the phenoxy radical formed from anisole (methoxybenzene) gave CO and cyclopentadienyl radicals during pyrolysis at 950 °C. Based on kinetics [33, 34] and *ab initio* calculation [35, 36] results, a decomposition mechanism has been proposed that involves forming a fused bicyclic cyclopropanone intermediate followed by breaking a C-C bond of the three-membered ring and subsequent elimination of CO. As for catechol, Ledesma et al. [8] reported CO, cyclopentadiene, acetylene and other low MW products from pyrocatechol at 700–1000 °C (residence time: 0.4 s). With the proposed mechanisms reported for phenol, they explained the formation of these products with a mechanism wherein a hydroxyl-substituted phenoxy radical formed from pyrocatechol decomposes into CO and a cyclopentadienol-lyl radical, which is further converted into cyclopentadienone. The latter compound then decomposes into acetylene and CO.

On the other hand, there are no reports in the literature discussing gas formation from pyrogallol. A similar mechanism proposed for phenol and pyrocatechol would be involved in the formation of CO from pyrogallols. However, the higher gas formation reactivity of pyrogallol along with the CO_2 formation should be explained by the

mechanism. Additionally, we propose a gasification pathway via an *o*-benzoquinone, as illustrated in Fig. 8. Oxidation into benzoquinone is a feasible reaction for some hydroxylated phenols, as reported in the studies of unimolecular decomposition of *p*- and *o*-hydroquinones mainly conducted by Dellinger's group [9, 38, 39]. Lomnicki et al. [9] reported that *p*-hydroquinone gave *p*-benzoquinone in a 32% yield at 550 °C, while *o*-benzoquinone was not observed as a product from *o*-hydroquinone (pyrocatechol). Such difference has been discussed with the influence of the position of hydroxyl group (*p*- or *o*-) on formation of semiquinone radicals as intermediates of benzoquinones [38, 40, 41].

Although the MeOH-soluble fractions from pyrocatechol (**2**) and 4-methylcatechol (**4**) were yellow, pyrogallol (**6**) gave red-colored solutions at 80 and 120 s, which were decolorized at a longer heating time of 600 s (Fig. 5). These red-colored solutions may arise from the *o*-benzoquinone type structures formed from pyrogallol (**6**), since *o*-benzoquinones are generally red-colored substances, while *p*-benzoquinones are yellow. Syringol (**16**), 3-methoxycatechol (**3**), 2-methoxy-6-methylphenol (**9**) and 3-methylcatechol (**5**) also gave red-colored solutions during the early stage of pyrolysis.

The calculated bond dissociation energy (BDE) of 68.1 kcal/mol (under AM1, B3LYP/6-311++G** level with a software "Spartan", zero-point correction) suggests that the C-C bond of the bicinal >C=O group in 3-hydroxy-*o*-benzoquinone (**17**) is cleaved homolytically at 600 °C. The resulting radical **18** may decompose into CO and a butadiene radical. Alternatively, addition of OH radical to **18** can form a carboxylic acid, which is further decomposed into CO_2. The CO_2 formation and higher gas formation reactivity of pyrogallol than pyrocatechol may be related to such pyrogallol-characteristic pathway, although further study is necessary regarding the formation and decomposition of *o*-benzoquinone **17** from pyrogallol.

3.5. GC/MS-detectable tar

Fig. 9 shows the time-dependent changes of the yields of GC/MS-detectable low MW tar components. Cresols/xylenols **8**, **10**–**13** and 2-ethylphenol (**14**) formed large amounts (15.9–38.9 wt%, 600 s) of these products but the yields from catechols/pyrogallols **2**, **4**–**7** were very low 0.4–3.0 wt%, 600 s. These results suggest that cresols/xylenols are the major sources of the low MW tar components at relatively long heating times, while catechols/pyrogallols contribute little. Although trace amounts of phenol, cresols and xylenols were identified in GC/MS analysis, the major components from catechols/pyrogallols were PAHs, as discussed below.

The products from cresols/xylenols **8**, **10**–**13** and 2-ethylphenol (**14**) are summarized in Table 1. Demethylation was observed as a major reaction. For example, *o*-cresol (**8**) and 2-ethylphenol (**14**) gave phenol in 18.0 and 20.7 wt%, respectively, at 600 s. Demethylation of alkylphenols has been reported in many papers under pyrolysis conditions [42–47]. Small amounts of *p*-cresol and *o*,*o*- and *o*,*p*-xylenols from *o*-cresol would be formed by coupling of the methyl radical with carbon-centered radicals rearranged from the phenoxy radical. *o*,*m*-Xylenols may be formed by a similar coupling

reaction with a carbon-centered radical rearranged from the benzyl radical. *o*-Cresol formation from 2-ethylphenol [2.8 (120 s) and 4.7 (600 s) wt%] indicates the C-C-bond cleavage in the ethyl group of **14**. Zhou and Crynes [46] reported similar C-C bond cleavage of the ethyl group under high pressure conditions. From the yields of these products, the reactivity was suggested to be greater in the order: demethylation > methylation, ethyl C-C bond cleavage.

From the results of xylenols **10**–**12** and trimethylphenol **13**, the demethylation reactivity can be discussed with regard to the position (*o*-, *m*- or *p*-) of the methyl group. 2,3-Xylenol (**10**) gave *m*-cresol in higher yield (32.6 wt%) than *o*-cresol (1.4 wt%). This indicates that the demethylation reactivity is higher at the *o*- than at the *m*-position. Higher reactivities of *o*- and *p*-methyl groups were also reported in the literature [16, 43, 44, 46]. As for the reactivities of *o*- and *p*-methyl groups, relative yields of *p*-/*o*-cresols (12.9/6.2) from 2,4-xylenol (**11**) and *o*,*p*-/*o*,*o*-xylenols (5.6/1.5) from trimethylphenol **13** [number in parenthesis: yield (wt%)] indicate that the *o*-methyl group is more reactive than the *p*-methyl group. Masuku [43] and Buryan [44] also reported similar relative reactivities.

Although many papers describe such demethylation reactions [16, 42–46], no reasonable mechanism has been presented. We present two possible mechanisms in Fig. 10, that is, direct hydrogen-transfer and radical coupling mechanisms. Both mechanisms form a methyl radical that is further converted into methane. The methane formation described above supports the existence of the methyl radical as the precursor.

Many papers [47–49] describe the hydrogen-transfer reaction in the aromatic ring during coal liquefaction in H-donor solvents such as tetralin (1,2,3,4–tetrahydronaphthalene), which is followed by cleavage of the strong bond between the aromatic ring and the aliphatic side-chain. We described H_2 formation from coke fractions prepared by pyrolysis of guaiacol/syringol (600 °C/ 80 s) [20]. Thus, the coking reaction would act as an H-donor (Fig. 10 a). Coke precursors may include similar reactive structures to H-donor solvents. Through this mechanism, higher reactivity of the *o*- and *p*-methyl groups is reasonably explained by the relative stabilities of the intermediate cyclohexandienyl radicals. Attack at the *o*-position will form a more stable radical than at the *m*-position [50]. One resonance structure has the radical on the carbon atom adjacent to the OH group and this stabilizes the radical [51]. Similar stabilization is expected for the *p*-methylated phenols but not for the *m*-methylated phenols.

Selectivity between *o*- and *p*-positions is explainable with the electrophilicity of the hydrogen radical. Addition of a radical to a double-bond carbon is known to be governed by several factors, including the polarity of these reactants [50]. An electrophilic radical prefers to add to a nucleophilic carbon, while a nucleophilic radical tends to add to an electrophilic carbon. Delbecq et al. [52] discussed the electrophilicity/nucleophilicity of the hydrogen radical for addition reactions to ethylene, vinylamine and vinylborane. They reported that the hydrogen radical acts as an electrophilic radical for ethylene and vinylamine with the N lone pair but as a

nucleophilic radical for vinylborane with a vacant orbital on the boron atom. According to their conclusion, the hydrogen radical is expected to act as an electrophilic radical for cresols/xylenols with the oxygen lone pair, which may assist the attack by the electrophilic hydrogen radical on the *o*-carbon.

Fig. 10 b shows a radical coupling mechanism including the coupling of phenoxy and hydrogen radicals. Phenoxy radical formation under the present conditions is supported by the coupling products with the methyl radical as described above. This coupling reaction forms a cyclohexadienone radical, which has a weaker C-CH_3 bond (calculated BDEs: 60.3 and 62.5 kcal/mol for *o*- and *p*-derivatives, respectively, under AM1, B3LYP/6-311++G** level with a software "Spartan", zero-point correction) than the corresponding phenols (110.5 and 106.7 kcal/mol). A similar influence of the conjugated carbonyl group has been reported for the β-ether cleavage of guaiacylglycerol-β-guaiacyl ether as a lignin model dimer [53]. The C_β-O bond homolysis temperature was lowered by 100 °C in a quinonemethide intermediate. Resonance structures of the phenoxy radical (migration into *o*- and *p*-carbons) explain the preferential demethylation at the *o*- and *p*-positions.

In both mechanisms, a hydroxyl group on the aromatic ring enhances the demethylation reactivity. This is confirmed by the very low reactivity of 1,3,5-trimethylbenzene (almost recovered at 600 °C/ 600 s). Further study is necessary to confirm these mechanisms and their contributions.

3.6. PAH

Biphenyl, xanthenes, naphthalene, 1-methylnaphthalene, 3-methylnaphthalene, phenanthrene and anthracene were identified as the major PAHs. These were also reported from guaiacol/syringol [20]. Fig. 11 summarizes their yields from phenol (**1**), 2-ethylphenol (**14**), catechols/pyrogallols **2**, **4**–**7** and cresols/xylenols **8**, **10**–**13** at 600 s. Their formation behaviors varied depending on the chemical structure of the intermediates. Catechols/pyrogallols tend to form biphenyl, naphthalenes and phenanthrene more selectively, while cresols/xylenols formed xanthene and anthracene preferentially. The yields from the syringol-characteristic pyrogallols **6** and **7** were particularly low. On the other hand, the guaiacol-characteristic pyrocatechol (**2**) and *o*-cresol (**8**) produced significant amounts of PAH. These are consistent with the earlier observation [20] that syringol produced less PAH than guaiacol under similar conditions. Naphthalenes from catechols **2**,**4** and **5** would be explained by the proposed mechanism, which includes the coupling of two cyclopentadienyl radicals formed from catechol and subsequent rearrangement into naphthalene [28-30].

Some correlation was observed for the yields of PAHs with two and three aromatic rings. The yields of phenanthrene and anthracene tend to be synchronized with those of biphenyl and xanthene, respectively. Because there are some structural similarities between the biphenyl-phenanthrene and xanthene-anthracene pairs (Fig. 12),

each pair of two and three aromatic ring PAHs would be formed through a common pathway.

3.7. Roles of intermediates in guaiacol and syringol pyrolysis

Fig. 13 illustrates the tar, gas and coke formation behaviors from guaiacol and syringol at 600 °C, as discussed with the reactivities of the intermediates suggested by the present study and our previous paper [20]. Table 2 also summarizes the roles of the intermediates in product formation. Pyrolytic reaction starts from the homolytic cleavage of the O-CH_3 bond [20], which gives CH_4 and catechols/pyrogallols through H-abstraction of the resulting radicals. The methyl radical also gives methylated aromatic compounds through radical coupling reactions [20]. High MW products are also formed. Such H-abstraction from the phenolic hydroxyl groups of guaiacol and syringol initiates a radical-induced rearrangement reaction to form cresols/xylenols. In the course of this rearrangement, coke (1st stage) is formed via *o*-quinonemethide intermediates. Demethoxylated products, that is, phenol and guaiacol from guaiacol and syringol, respectively, are also produced through decarbonylation (CO formation) of the aldehyde intermediates [20]. Phenol is quite stable at 600 °C.

Following these initial reactions, catechols/pyrogallols then decomposed to form CO (additionally CO_2 in the case of pyrogallols) and a small amount of coke. On the other hand, the cresols/xylenols decomposition occurs later with the lower reaction rates, which includes demethylation to form CH_4, H_2, phenol and cresols with coke (2nd stage). CH_4, H_2 and coke formation also proceeds in catechols/pyrogallols at this stage. As the pyrolysis progresses, 1st stage coke is gasified into H_2, CO and CO_2, while the 2nd stage coke is formed from catechols/pyrogallols and cresols/xylenols. The 2nd stage coking is accompanied by PAH formation. Biphenyl, naphthalenes and phenanthrene are formed more selectively from catechols/xylenols. In contrast, xanthene and anthracene are formed from cresols/xylenols.

Table 3 summarizes the characteristic features of syringol and guaiacol at 600 °C. Syringol, with an additional OCH_3 group, produces more 1st stage coke and CH_4 [20]. This reduces the amounts of low MW intermediates. The pyrolytic intermediates from syringol, with more OH and CH_3 substituents, have generally higher decomposition reactivities. In particular, higher gasification reactivities of pyrogallols into CO and CO_2 would be a reason for the higher gasification reactivity of syringol. Only pyrogallols form CO_2 in substantial yields. Accordingly, the CH_4 and CO_2 yields are greater from syringol, as reported in the previous paper [20].

Conclusions

Thermal reactivities of the pyrolysis intermediates generated from guaiacol and syringol were clarified at 600 °C in a closed ampoule reactor. The reactivity increased with an increase in the number of OH and CH_3 groups on the aromatic ring and the

enhancing effects were greater for OH than CH_3. Accordingly, catechols/pyrogallols formed through O-CH_3 bond homolysis generally exhibited higher reactivities than cresols/xylenols, formed through a radical-induced rearrangement reaction. These reactivity differences are consistent with the rapid disappearance of catechols/pyrogallols during pyrolysis of guaiacol and syringol. Phenol was quite stable under the present conditions.

As for the roles of the intermediates during product formation, the following features were clarified. Aromatic O-CH_3 is a key structure during early stage 1st stage coking, while most of the intermediates used in this study other than phenol and 2-ethylphenol were active during the 2nd stage coking. Interestingly, the ethyl group was not effective for this coking and this suggests that methyl groups in cresols/xylenols are important structures for the coking reactions involving these intermediates. Catechols/pyrogallols were effectively converted into CO and CO_2 (in the case of pyrogallols) in relatively early stages of the pyrolysis. On the other hand, gas (H_2 and CH_4) formation from cresols/xylenols occurred later, with a lower reactivity. Demethylation was a principle reaction in this conversion and gave demethylation products (phenol and cresols) in substantial yields. The demethylation reaction, which occurred preferentially at the *o*- and *p*-positions of the OH group, was discussed in the light of possible reaction mechanisms. A gas formation mechanism, which involves an *o*-benzoquinone intermediate, was also presented.

Acknowledgments

This work was supported by a Grant-in-Aid for Scientific Research (B)(2) (No. 203801035007, 2008.4-2011.3) and the Kyoto University Global COE program for "Energy Science in the Age of Global Warming".

References

[1] J. Zakzeski, P. C. A. Bruijnincx, A. L. Jongerius, B. M. Weckhuysen, Chem. Rev. 110 (2010) 3552.
[2] R. J. Evans, T. A. Milne, M. N. Soltys, J. Anal. Appl. Pyrol. 9 (1986) 207.
[3] C. Saiz-Jimenez, J. W. De Leeuw, Org. Geochem. 10 (1986) 869.
[4] O. Faix, D. Meier, I. Grobe, J. Anal. Appl. Pyrol. 11 (1987) 403.
[5] W. Genuit, J. J. Boon, O. Faix, Anal. Chem. 59 (1987) 508.
[6] P. F. Greenwood, J. D. H. van Heemst, E. A. Guthrie, P. G. Hatcher, J. Anal. Appl. Pyrol. 62 (2002) 365.
[7] J. R. Obst, J. Wood Chem. Technol. 3 (1983) 377.
[8] E. B. Ledesma, N. D. Marsh, A. K. Sandrowitz, M. J. Wornat, P. Combust. Inst. 29 (2002) 2299.
[9] S. Lomnicki, H. Truong, B. Dellinger, Chemosphere 73 (2008) 629.
[10] E. J. Shin, M. R. Hajaligol, R. Rasouli, Fuel 83 (2004) 1445.

[11] R. Cypres, B. Bettens, Tetrahedron 31 (1975) 53.
[12] L. Khachatryan, J. Adounkpe, Z. Maskos, B. Dellinger, Environ. Sci. Technol. 40 (2006) 5071.
[13] P. Zhou, B. L. Crynes, Ind. Eng. Chem. Process Des. Dev. 25 (1986) 898.
[14] R. Nakai, Bull. Chem. Soc. Jpn. 5 (1930) 136.
[15] R. Wandas, J. Surygała, E. Śliwka, Fuel 75 (1996) 687.
[16] B. W. Jones, M. B Neuworth, Ind. Eng. Chem. 44 (1952) 2872.
[17] C. P. Masuku, Fuel 71 (1992) 503.
[18] E. Dorrestijn, P. Mulder, J. Chem. Soc., Perkin Trans. 2 (1999) 777.
[19] M. Asmadi, H. Kawamoto, S. Saka, J. Wood Sci. 56 (2010) 319.
[20] M. Asmadi, H. Kawamoto, S. Saka, J. Anal. Appl. Pyrol. submitted.
[21] T. Hosoya, H. Kawamoto, S. Saka, J. Anal. Appl. Pyrol. 84 (2009) 79.
[22] T. Hosoya, H. Kawamoto, S. Saka, J. Anal. Appl. Pyrol. 83 (2008) 71.
[23] T. Hosoya, H. Kawamoto, S. Saka, J. Anal. Appl. Pyrol. 78 (2007) 328.
[24] N. D. Marsh, E. B. Ledesma, A. K. Sandrowitz, M. J. Wornat, Energ. Fuel 18 (2004) 209.
[25] W. J. Wornat, E. B. Ledesma, N. D. Marsh, Fuel 80 (2001) 1711.
[26] E. B Ledesma, N. D. Marsh, A. K. Sandrowitz, M. J. Wornat, Energ. Fuel 16 (2002) 1331.
[27] R. Cypress, B. Bettens, Tetrahedron 31 (1975) 359.
[28] N. M. Marinov, W. J. Pitz, C. K. Westbrook, A. M. Vincitore, M. J. Castaldi, S. M. Senkan, Combust. Flame 114 (1998) 192.
[29] N. M. Marinov, W. J. Pitz, C. K. Westbrook, M. J. Castaldi, S. M. Senkan, Combust. Sci. Technol. 116-117 (1996) 211.
[30] C. F. Melius, M. E. Colvin, N. M. Marinov, W. J. Pitz, S. M. Senkan, Symp. Int. Combust. 26 (1996) 685.
[31] K. Brezinsky, M. Pecullan, I. Glassman, J. Phys. Chem. 102 (1998) 8614.
[32] A. B. Lovell, K. Brezinsky, I. Glassman, Int. J. Chem. Kinet. 21 (1989) 547.
[33] A. J. Colussi, F. Zabel, S. W. Int. J. Chem. Kinet. 9 (1977) 161.
[34] C. Y. Lin, M. C. Lin, J. Phys. Chem. 90 (1996) 425.
[35] R. Liu, K. Morokuma, A. M. Mebel, M. C. Lin, J. Phys. Chem. 100 (1996) 9314.
[36] S. Olivella, A. Solé, A García-Raso, J. Phys. Chem. 99 (1995) 10549.
[37] A. G. Harrison, L. R. Honnen, H. J. Dauben Jr, F. P. Lossing, J. Am. Chem. Soc. 82 (1960) 5593.
[38] L. Khachatryan, R. Asatryan, C, McFerrin, J. Adounkpe, Z. Maskos, B. Dellinger, J. Phys. Chem. 114 (2010) 10110.
[39] L. Khachatryan, J. Adounkpe, R. Asatryan, B. Dellinger, J. Phys. Chem. 114 (2010) 2306.
[40] J. Adounkpe, L. Khatchatryan, B. Dellinger, Energ. Fuel 22 (2008) 2986.
[41] M. Altarawneh, B. Z. Dlugogorski, E. M. Kennedy, J. C. Mackie, J. Phys. Chem. 114 (2010) 1060.

[42] R. Cypres, B. Bettens, Tetrahedron 30 (1974) 1253.
[43] C. P. Masuku, Fuel 71 (1992) 503.
[44] P. Buryan, J. Anal. Appl. Pyrol. 22 (1991) 83.
[45] P. Zhou, B. L. Crynes, Ind. Eng. Chem. Process Des. Dev. 25 (1986) 898.
[46] R. Nakai, Bull. Chem. Soc. Jpn. 5 (1930) 136.
[47] D. F. McMillen, R. Malhotra, G. P. Hum, S. J. Chang, Energ. Fuel 1 (1987) 193.
[48] D. F. McMillen, R. Malhotra, J. Chang, W. C. Ogier, S. E. Nigenda, R. H. Fleming, Fuel 66 (1987) 1611.
[49] R. Malhotra, D. F. McMillen, Energ. Fuel 4 (1990) 184.
[50] A. F. Parsons, An introduction to free radical chemistry, Blackwell Science, Oxford, 2000, pp. 67-70.
[51] D. J. Pasto, R. Krasnansky, C. Zercher, J. Org. Chem. 52 (1987) 3062.
[52] F. Delbecq, D. Ilavsky, N. T. Anh, J. M. Lefour, J. Am. Chem. Soc. 107 (1985) 1623.
[53] T. Nakamura, H. Kawamoto, S. Saka, Holzforschung 62 (2008) 50.

Figure Legends

Fig. 1 Lignin pyrolysis intermediates used in this study.

Fig. 2 Time-dependent changes in the recovery of compounds **1**, **2**, **4**–**8**, **10**–**14** during pyrolysis at 600 °C in N_2 for 80–600 s.

Fig. 3 Yields of gas, MeOH-soluble and MeOH-insoluble (coke) fractions during pyrolysis at 600 °C in N_2 for 80–600 s. *White*: gas; *grey*: MeOH-soluble; *black*: MeOH-insoluble (coke).

Fig. 4 Influences of temperature on gas yield during pyrolysis of pyrocatechol (**2**), pyrogallol (**6**), *o*-cresol (**8**) and 2,6-xylenol (**12**) (N_2/ 400–600 °C/ 120 s).

Fig. 5 Pictures of the ampoule reactors after tar extraction and the MeOH-soluble tar fractions obtained after pyrolysis of compounds **1**–**16** (N_2/ 600 °C/ 40–600 s). [a] Ref. [41].

Fig. 6 *o*-Quinonemethide and coke formation from methylated phenol.

Fig. 7 Yields of gaseous products during pyrolysis of various lignin pyrolysis intermediates (N_2/ 600 °C/ 80–600 s). *Cross*: phenol (**1**); *solid circle*: pyrocatechol (**2**); *solid square*: 4-methylcatechol (**4**); *open circle*: pyrogallol (**6**); *open square*: 5-methylpyrogallol (**7**); *solid triangle*: *o*-cresol (**8**); *solid diamond*: 2,4-xylenol (**11**); *open triangle*: 2,6-xylenol (**12**); *open diamond*: 2,4,6-trimethylphenol (**13**).

Fig. 8 A possible mechanism for gas formation from pyrogallol (**6**) via an *o*-quinone intermediate. [a] Calculated bond dissociation energy (kcal/mol, under AM1, B3LYP/6-311++G** level with a software "Spartan", zero-point correction).

Fig. 9 Total yields of GC/MS-detectable tar components (excluding starting compound) from various lignin pyrolysis intermediates (N_2/ 600 °C/ 80–600 s). *Solid circle*: phenol (**1**); *solid square*: pyrocatechol (**2**); *solid triangle*: 4-methylcatechol (**4**); *solid diamond*: 3-methylcatechol (**5**), *open square*: pyrogallol (**6**); *open triangle*: 5-methylpyrogallol (**7**); *inverted-solid triangle*: *o*-cresol (**8**); *inverted-open triangle*: 2,3-xylenol (**10**); *open diamond*: 2,4-xylenol (**11**); *pentagon*: 2,6-xylenol (**12**); *cross*: 2,4,6-trimethylphenol (**13**); *open circle*: 2-ethylphenol (**14**).

Fig. 10 Proposed direct hydrogen-transfer and radical coupling mechanisms for demethylation of cresols/xylenols. [a] Bond dissociation energy (kcal/mol, under AM1, B3LYP/6-311++G** level with a software "Spartan", zero-point correction).

Fig. 11 Yields of PAHs from phenols **1**, **14**, catechols/pyrogallols **2**, **4**–**7** and cresols/xylenols **8**, **10**–**13** (N_2/ 600 °C/ 600 s). [a] total yield of naphthalene, 1-methylnaphthalene and 2-methylnaphthalene.

Fig. 12 Structural similarities between biphenyl/phenanthrene and xanthene/anthracene pairs.

Fig. 13 Roles of pyrolysis intermediates in tar, gas and coke formation from guaiacol and syringol (N_2/ 600 °C).

Table Captions

Table 1 Yields (wt%) of GC/MS-detectable products from *o*-cresol (**8**), xylenols (**10**–**12**), trimethylphenol (**13**) and 2-ethylphenol (**14**) (N_2/ 600 °C/ 120–600 s).

Table 2 Roles of intermediates in pyrolytic formation of various products from guaiacol and syringol (N_2/ 600 °C).

Table 3 Comparison of the pyrolytic reactivities of syringol and guaiacol at 600 °C.

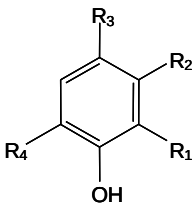

	R_1	R_2	R_3	R_4
1	H	H	H	H
2	OH	H	H	H
3	OH	H	H	OCH_3
4	OH	H	CH_3	H
5	OH	H	H	CH_3
6	OH	H	H	OH
7	OH	H	CH_3	OH
8	CH_3	H	H	H
9	OCH_3	H	H	CH_3
10	CH_3	CH_3	H	H
11	CH_3	H	CH_3	H
12	CH_3	H	H	CH_3
13	CH_3	H	CH_3	CH_3
14	CH_2CH_3	H	H	H

Fig. 1 Lignin pyrolysis intermediates used in this study.

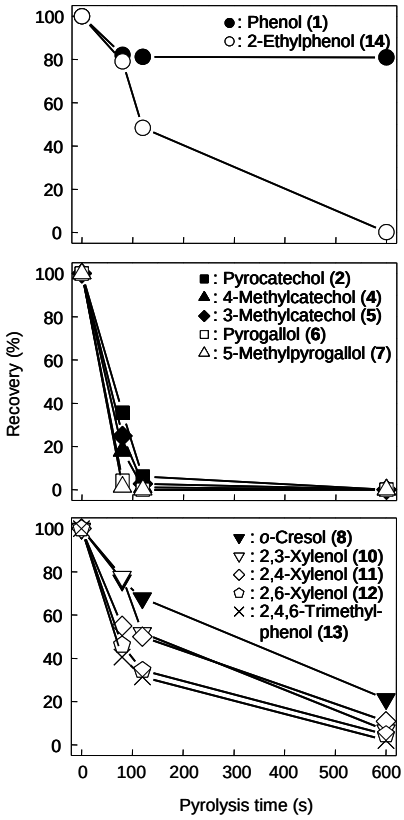

Fig. 2 Time-dependent changes in the recovery of compounds **1**, **2**, **4**–**8**, **10**–**14** during pyrolysis at 600 °C in N_2 for 80–600 s.

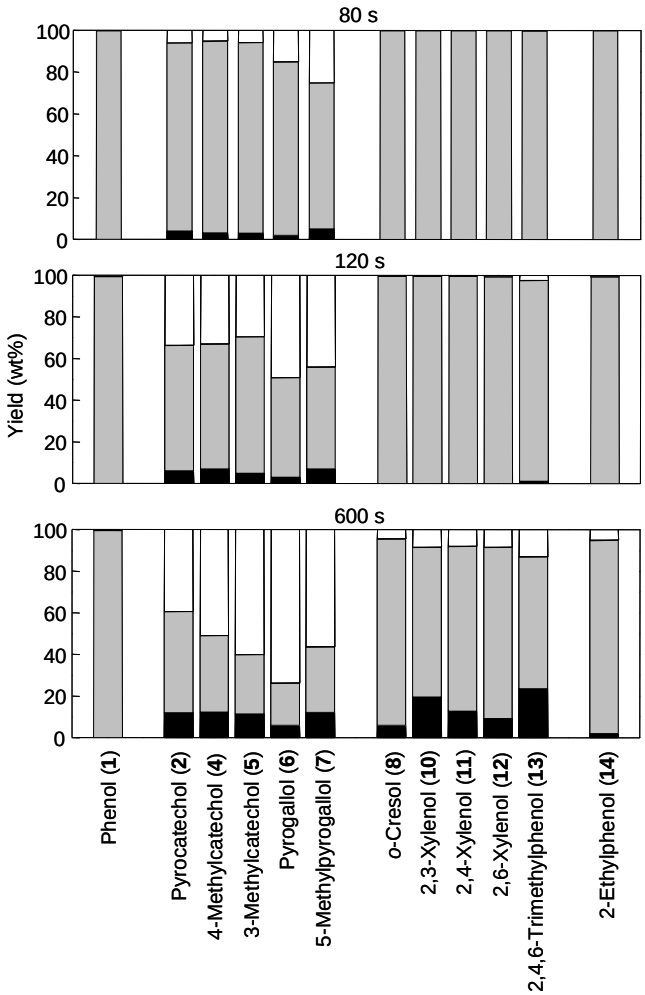

Fig. 3 Yields of gas, MeOH-soluble and MeOH-insoluble (coke) fractions during pyrolysis at 600 °C in N_2 for 80–600 s. *White*: gas; *grey*: MeOH-soluble; *black*: MeOH-insoluble (coke).

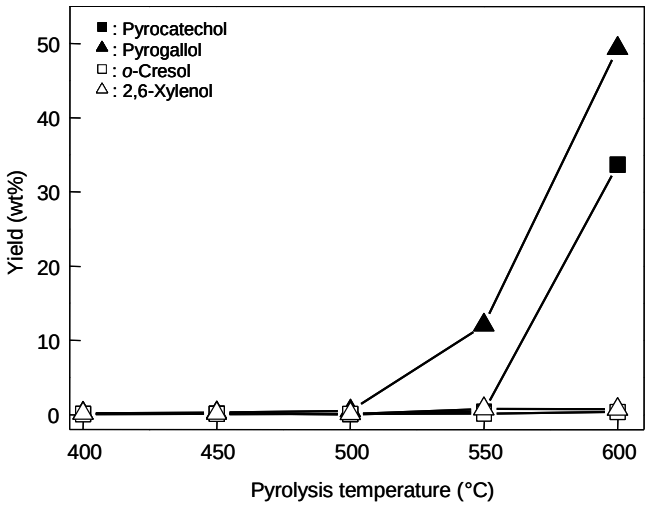

Fig. 4 Influences of pyrolysis temperature on gas yield during pyrolysis of pyrocatechol (**2**), pyrogallol (**6**), *o*-cresol (**8**) and 2,6-xylenol (**12**) (N_2/ 400–600 °C/ 120 s).

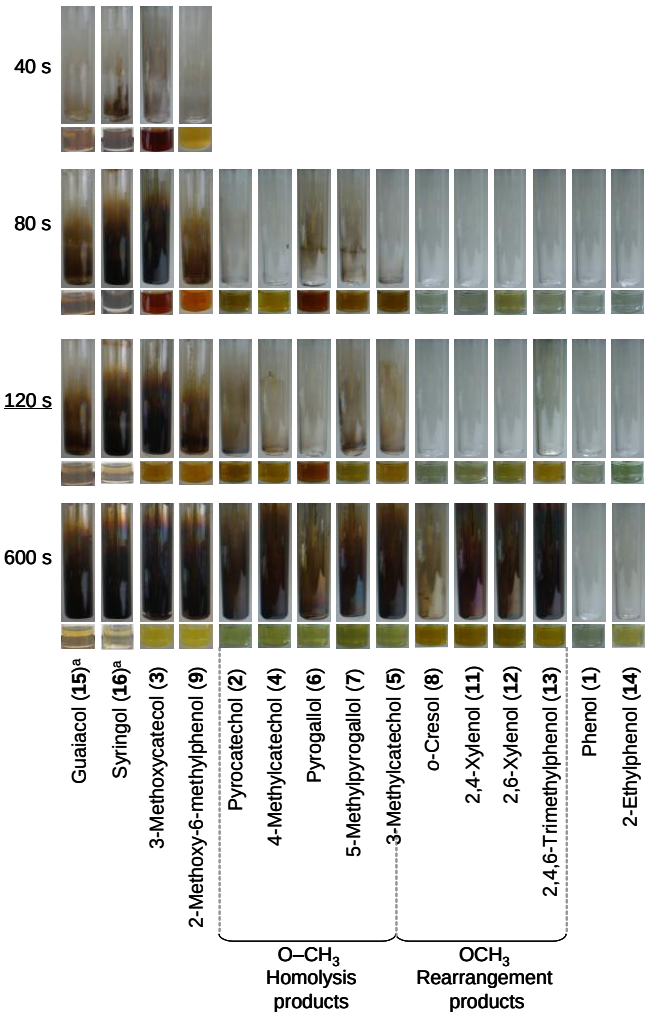

Fig. 5 Pictures of the ampoule reactors after tar extraction and the MeOH-soluble tar fractions obtained after pyrolysis of compounds **1**–**16** (N_2/ 600 °C/ 40–600 s). [a] Ref. [20].

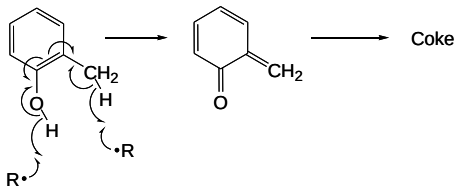

Fig. 6. *o*-Quinonemethide and coke formation from methylated phenol.

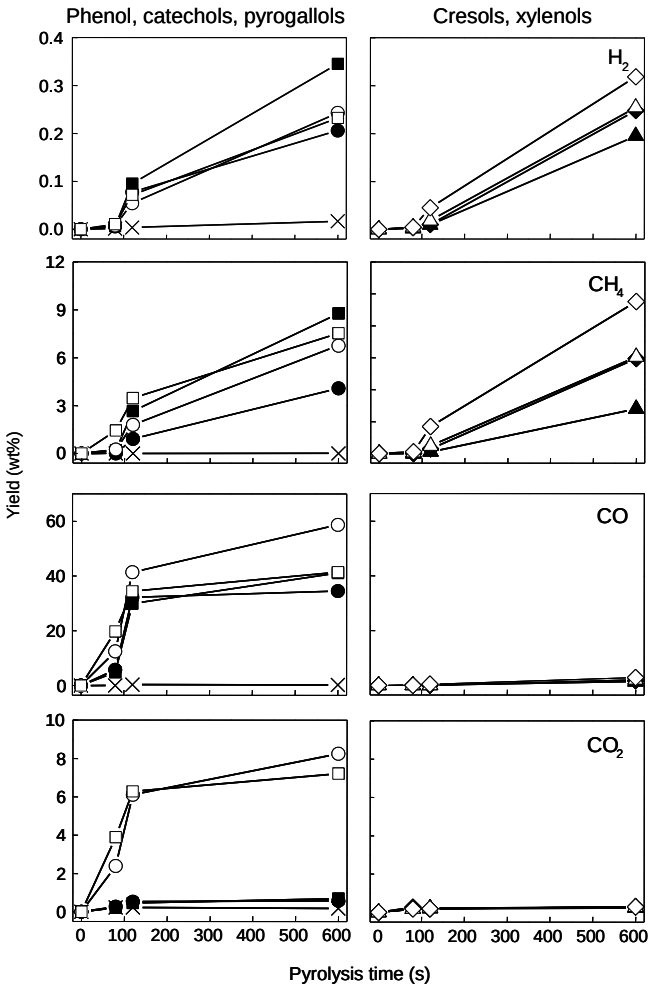

Fig. 7 Yields of gaseous products during pyrolysis of various lignin pyrolysis intermediates (N_2/ 600 °C/ 80–600 s). *Cross*: phenol (**1**); *solid circle*: pyrocatechol (**2**); *solid square*: 4-methylcatechol (**4**); *open circle*: pyrogallol (**6**); *open square*: 5-methylpyrogallol (**7**); *solid triangle*: *o*-cresol (**8**); *solid diamond*: 2,4-xylenol (**11**); *open triangle*: 2,6-xylenol (**12**); *open diamond*: 2,4,6-trimethylphenol (**13**).

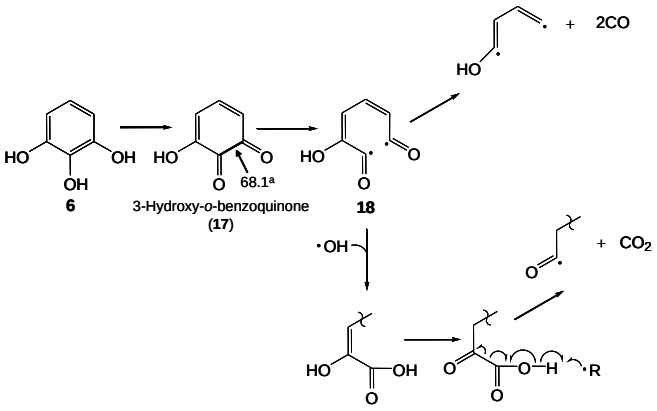

Fig. 8 A possible mechanism for gas formation from pyrogallol (**6**) via an *o*-quinone intermediate. [a] Calculated bond dissociation energy (kcal/mol, under AM1, B3LYP/6-311++G** level with a software "Spartan", zero-point correction).

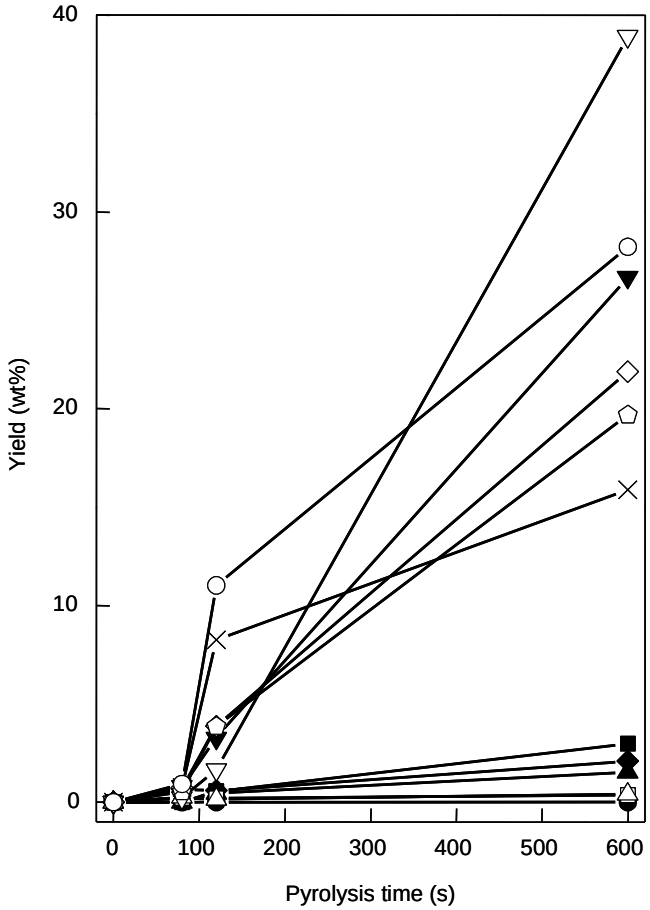

Fig. 9 Total yields of GC/MS-detectable tar components (excluding starting compound) from various lignin pyrolysis intermediates (N_2/ 600 °C/ 80–600 s). *Solid circle*: phenol (**1**); *solid square*: pyrocatechol (**2**); *solid triangle*: 4-methylcatechol (**4**); *solid diamond*: 3-methylcatechol (**5**), *open square*: pyrogallol (**6**); *open triangle*: 5-methylpyrogallol (**7**); *inverted-solid triangle*: *o*-cresol (**8**); *inverted-open triangle*: 2,3-xylenol (**10**); *open diamond*: 2,4-xylenol (**11**); *pentagon*: 2,6-xylenol (**12**); *cross*: 2,4,6-trimethylphenol (**13**); *open circle*: 2-ethylphenol (**14**).

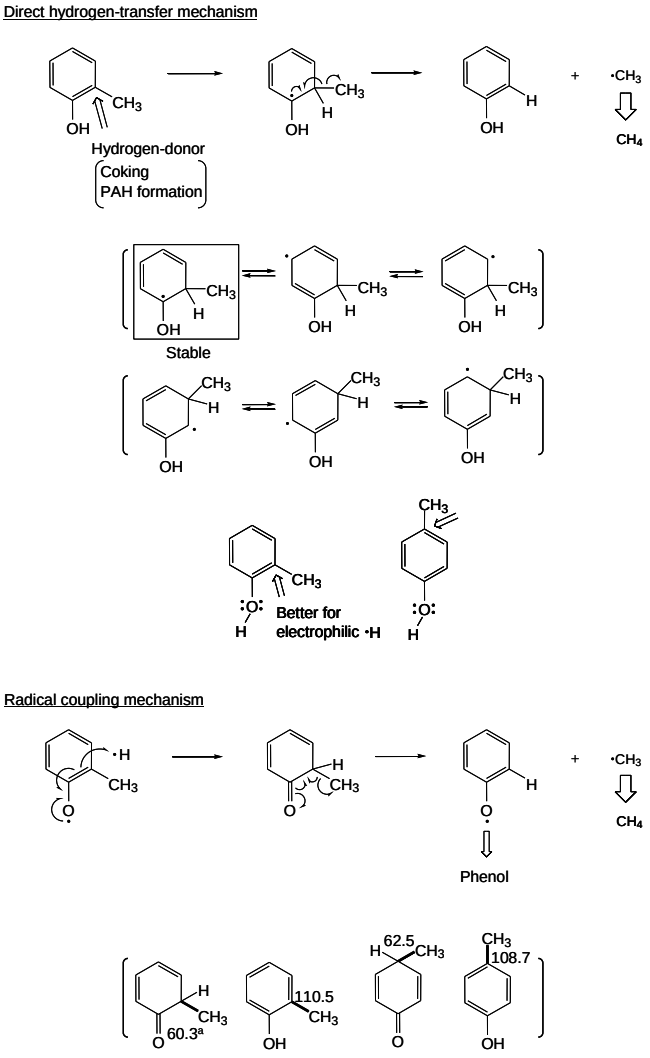

Fig. 10 Proposed direct hydrogen-transfer and radical coupling mechanisms for demethylation of cresols/xylenols. [a] Calculated bond dissociation energy (kcal/mol, under AM1, B3LYP/6-311++G** level with a software "Spartan", zero-point correction.

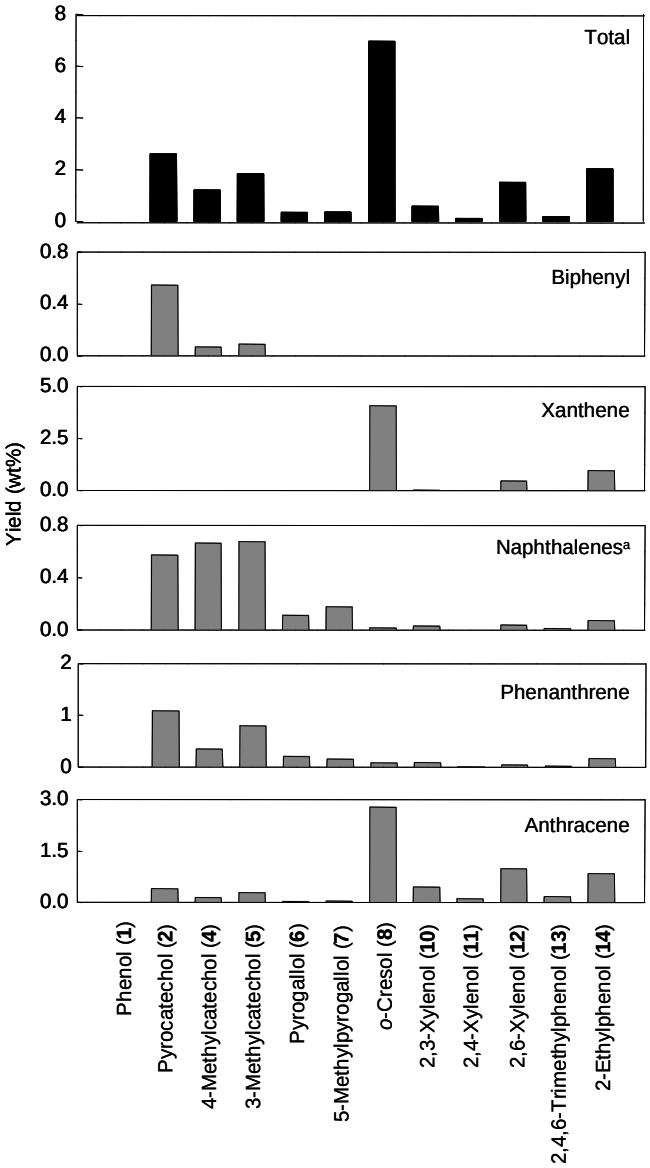

Fig. 11 Yields of PAHs from phenols **1**, **14**, catechols/pyrogallols **2**, **4**–**7** and cresols/xylenols **8**, **10**–**13** (N_2/ 600 °C/ 600 s). [a] Total yield of naphthalene, 1-methylnaphthalene and 2-methylnaphthalene.

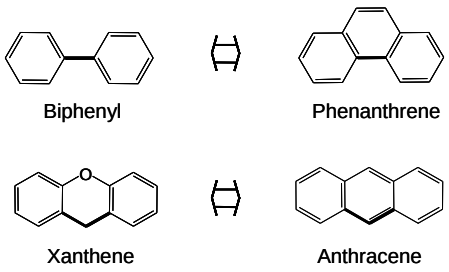

Fig. 12 Structural similarities between biphenyl/phenanthrene and xanthenes/ anthracene pairs.

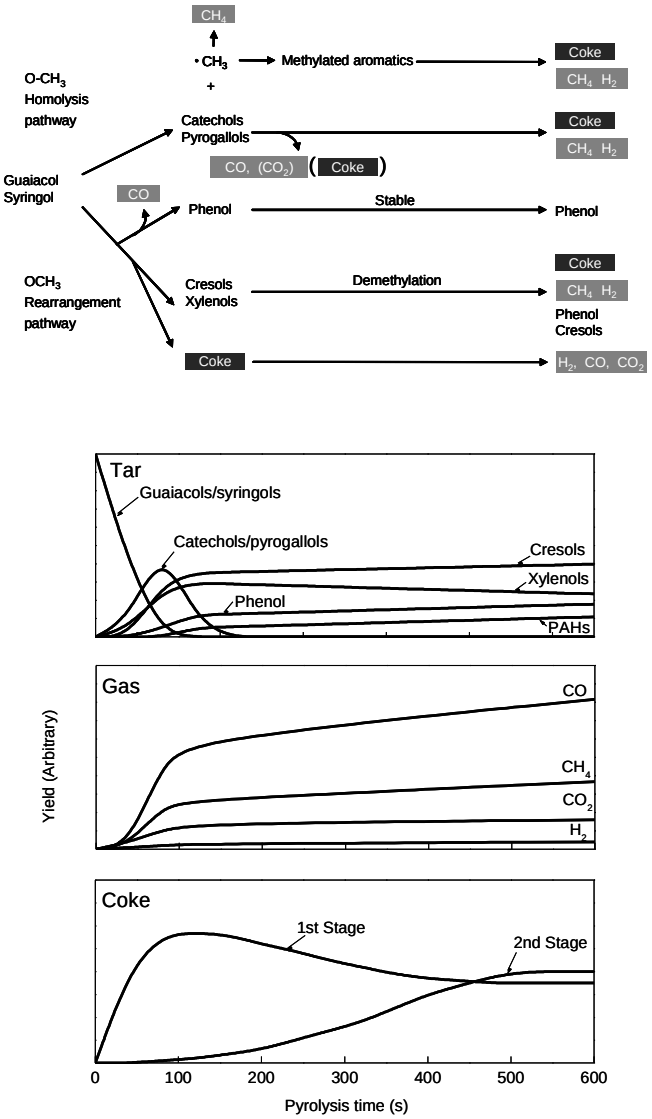

Fig. 13 Roles of pyrolysis intermediates in tar, gas and coke formation from guaiacol and syringol (N_2/ 600 °C).

Table 1
Yields (wt%) of the GC/MS-detectable products from *o*-cresol (**8**), xylenols (**10–12**), trimethylphenol (**13**) and 2-ethylphenol (**14**) (N_2/ 600 °C/ 120–600 s).

Starting compound	Pyrolysis time (s)	Cresols			Xylenols						Phenol
		o–	*m*–	*p*–	*o, m*– (2, 3)	*o, m*– (2, 5)	*o, p*–	*o, o*–	*m, m*–	*m, p*–	
o-Cresol (**8**)	120	S [a]	_ [b]	–	–	0.02	–	1.2	_	_	1.9
	600	S	_	0.38	0.03	0.11	0.04	1.0	_	_	18.0
2-Ethylphenol (**14**)	120	2.8	–	0.2	–	–	–	–	–	–	7. 8
	600	4.7	–	0.2	–	–	–	–	–	–	20.7
2, 3-Xylenol (**10**)	120	0.03	1.5	–	S	_	0.19	–	_	_	0.0
	600	1.4	32.6	–	S	_	3.2	0.07	_	_	1.0
2, 4-Xylenol (**11**)	120	0.89	_	3.0	_	_	S	–	_	_	0.0
	600	6.2	_	12.9	_	_	S	0.27	_	_	2.4
2, 6-Xylenol (**12**)	120	3.7	_	0.01	–	–	0.14	S	_	_	0.0
	600	14.3	_	0.32	0.11	0.46	0.09	S	_	_	2.9
2, 4, 6-Trimethylphenol (**13**)	120	0.13	_	0.05	_	_	6.1	2.0	_	_	0.0
	600	4.5	_	3.3	_	_	5.6	1.5	_	_	0.8

[a] Starting compound
[b] Not detected

Table 2
Roles of intermediates in pyrolytic formation of various products from guaiacol and syringol (N_2/ 600 °C).

Products	Pyrolysis intermediates			
	Aromatics with OCH_3 [a]	Catechols/ pyrogallols	Cresols/ xylenols	1st Stage coke
Coke				
1st Stage	◎			
2nd Stage		◎	◎	
Gas				
CH_4	◎	○	○	
H_2		○	○	○
CO		◎		○
CO_2		◎		○
		(Pyrogallols)		
Tar				
Cresols/ phenol			◎	
PAHs				
Biphenyl		◎		
Naphthalenes		◎	△	
Phenanthrene		◎	△	
Xanthene			◎	
Anthracene		△	◎	

[a] This type exists only in the early stage of pyrolysis.

Table 3
Comparison of the pyrolytic reactivities of syringol and guaiacol at 600 °C.

	Relative reactivity of syringol as compared with that of guaiacol
Coking	
1st Stage	More extensive (Additional OCH_3 group)
Tar reactivity	More reactive (More substituents)
Gas formation	More reactive (Additional OCH_3 group; Higher intermediates reactivities)
Gas composition	More CH_4 and CO_2 (CH_4: additional OCH_3 group; CO_2: from pyrogallols)